CHAPTER 103

WAVE TRANSMISSION THROUGH PERMEABLE BREAKWATERS

by

Charles K. Sollitt, Asst. Professor
Oregon State University
Ralph H. Cross, Coastal Engineer
Alpine Geophysical Assocs., Inc.

Abstract

A theory is derived to predict ocean wave reflection and transmission at a permeable breakwater of rectangular cross section. The theory solves for a damped wave component within the breakwater and matches boundary conditions at the windward and leeward breakwater faces to predict the reflected and transmitted wave components. An approximate solution to conventional rubble mound breakwater designs is formulated in terms of an equivalent rectangular breakwater with an additional consideration for wave breaking. Experimental and theoretical results are compared and evaluated.

Introduction

It is common practice in coastal engineering design to account for wave transmission past rubble mound breakwaters by considering two possible transfer mechanisms: 1) diffraction through navigation openings in the structure, and 2) overtopping across the crest of the structure. Standard optical techniques have been modified to account for the diffraction process. The overtopping process is less well defined, however, recent semi-empirical methods (Cross, Sollitt, 1971) have improved design capabilities.

Both procedures are based on the assumption that the structure itself is impervious. However, field and laboratory observations raise some doubts about the universal applicability of this assumption. Calhoun (1971) has recorded transmission coefficients up to 40% resulting from the transmission of low crested swell directly through the pores of the rubble mound breakwater at Monterey Harbor, California. Similar observations have been reported by the New England Division, Army Corps of Engineers for the Isle of Shoals breakwater off the Maine-New Hampshire coast. This behavior is aggravated by long wave excitation and may be an important consideration in harbor seiching.

Neglecting the effect of direct transmission can be a significant omission in breakwater and harbor design. The analysis described in this study provides a technique which may be used to evaluate this important characteristic of permeable breakwaters.

Problem Statement

Wave interaction with permeable breakwaters excites wave motion within the interstices of the structure as well as producing reflected and transmitted waves. As an incident wave encounters a breakwater face part of the wave is reflected back out to sea, some energy is lost to wave breaking and the remaining energy is transmitted to the breakwater interior. The wave inside the structure decays as it propagates through the pores. Upon reaching the leeward face, the wave is partially transmitted to the lee side of the breakwater and is partially reflected back to the interior of the structure. This process yields two wave trains propagating in opposite directions within the structure, a reflected wave train propagating back out to sea and a transmitted wave train propagating beyond the lee side of the breakwater. In order to predict the characteristics of the wave which is ultimately transmitted beyond the breakwater, it is necessary to develop an analysis which properly identifies the reflected and interior wave motion as well.

The analytical approach used in this study begins with the unsteady equations of motion for flow in the pores of a coarse granular medium. The equations are linearized using a technique which approximates the turbulent damping condition inside the medium. This yields a potential flow problem satisfied by an eigen series solution. Linear wave theory is applied outside the breakwater and the excitation is provided by a monochromatic incident wave. The solutions are matched at the sea-breakwater interfaces by requiring continuity of horizontal mass flux and pressure. The amplitude and phase of the unknown wave components are solved from the latter boundary condition.

The Equations of Motion

A complete derivation of the theory is presented in a separate report by the authors (Sollitt, Cross, 1972). The major features are outlined herein.

The fluid motion in the interstices of the structure is described in terms of the seepage velocity and pressure. These are conceptual quantities which are averaged over finite and continuously destributed pore volumes. The incompressible equations of motion reduce to the following form:

$$\frac{\partial q}{\partial t} = -\frac{1}{\rho}\nabla (p + \gamma z) + \text{resistance forces}$$

$$\nabla \cdot q = 0 \qquad (1)$$

where q is the instanteous Eulerian velocity vector at any point, p is the corresponding pressure, γ is the fluid weight density, ρ is the fluid mass density, z is the vertical coordinate, t is time and ∇ is the gradient operator.

The gross effect of local spatial and temporal perturbations in the velocity field are accounted for by the resistance forces. The convective acceleration term is ignored because finite amplitude waves are quickly dissipated within coarse granular media.

The resistance forces in Eq. (1) are evaluated by combining known steady and unsteady stress relationships. Ward (1964) has demonstrated that under steady flow conditions the pressure drop through large grain permeable media is specified by

$$-\frac{1}{\rho}\nabla\,(p+\gamma z) = \frac{\nu}{K_p}\,\varepsilon q + \frac{C_f}{\sqrt{K_p}}\,\varepsilon^2\, q\,|q| \qquad (2)$$

where ν is the kinematic viscosity, K_p is the intrinsic permeability, C_f is a dimensionless turbulent resistance coefficient and ε is the porosity of the medium. The linear term governs low Reynolds number flow and the square law term dominates high Reynolds number flow.

In the present application, it is hypothesized that unsteadiness may be accounted for by introducing an additional term which evaluates the added resistance caused by the virtual mass of discrete grains within the medium. The resistance force due to the virtual mass is equal to the product of the displaced fluid mass, the virtual mass coefficient, and the acceleration in the approach velocity. The resulting force is distributed over the fluid mass within the pore so that the force per unit mass of fluid is simply

$$\frac{1-\varepsilon}{\varepsilon}\,C_M\,\frac{\partial q}{\partial t}$$

where C_M is the virtual mass coefficient of medium grains. C_M is a known quantity for isolated simple shapes, but generally is unknown for random, densely packed materials.

Combining the steady state damping law proposed by Ward with the additional inertial damping law proposed by the authors yields the appropriate replacement for the resistance forces in Eq. (1).

$$\frac{\partial q}{\partial t} = -\frac{1}{\rho}\nabla\,(p+\gamma z) - \frac{\nu}{K_p}\,\varepsilon q - \frac{C_f}{\sqrt{K_p}}\,\varepsilon^2\, q\,|q| - \frac{1-\varepsilon}{\varepsilon}\,C_M\,\frac{\partial q}{\partial t}$$

$$\nabla \cdot q = 0 \qquad (3)$$

The non dissipative inertial resistance term may be transposed to the left hand side of the equation and an inertial coefficient, S, defined as

$$S = 1 + \frac{1-\varepsilon}{\varepsilon}\,C_M \qquad (4)$$

then the equation of motion becomes

$$S\frac{\partial q}{\partial t} = -\frac{1}{\rho}\nabla(p+\gamma z) - \frac{\nu}{K_p}\varepsilon q - \frac{C_f}{\sqrt{K_p}}\varepsilon^2 q|q| \qquad (5)$$

$$\nabla \cdot q = 0$$

Note that Eq. (5) reduces to Darcy's Law for low Reynolds number, steady flow.

Linearzation Technique

In order to find an analytical solution to Eq. (5) some linearizing is necessary. The specific technique employed is as follows. The dissipative stress term in Eq. (5) is replaced by an equivalent stress term linear in q, i.e.,

$$\frac{\nu\varepsilon q}{K_p} + \frac{C_f\varepsilon^2}{\sqrt{K_p}} q|q| \rightarrow f\sigma q \qquad (6)$$

where σ is the angular frequency of the periodic motion and f is a dimensionless friction or damping coefficient. The coefficient σ is introduced to make f dimensionless and for subsequent algebraic expediency. To evaluate f in terms of the known damping law it is required that both the linear and non-linear friction laws account for the same amount of energy dissipation during one wave cycle. This is commonly referred to as Lorentz's condition of equivalent work.

The resistance term in the equation of motion, expressed in either form of Eq. (6) represents a friction force per unit mass acting at a point in the flow field. If this term is multiplied times the mass flux per unit volume flowing in a direction opposed to the friction force, the resulting quantity is the power dissipated per unit volume. If the power dissipation per unit volume is integrated over the volume of the flow field, ₩, and the wave period, T, the resulting quantity is the total energy consumed by friction in the volume of interest during one wave period. According to Lorentz's hypothesis, this quantity must be the same for all legitimate damping laws describing the same process. In equation form, this constraint is written

$$\int_{₩}\varepsilon d₩\int_{t}^{t+T} f\sigma q\cdot\rho q\,dt = \int_{₩}\varepsilon d₩\int_{t}^{t+T}\left\{\frac{\nu\varepsilon q}{K_p} + \frac{C_f\varepsilon^2}{K_p} q|q|\right\}\cdot\rho q\,dt$$

Thus a unique relationship exists between the medium parameters (ε, K_p, C_f), the flow field parameters (ν,q) and the friction coefficient, f. With f evaluated as a constant throughout $\forall$, this relationship may be written

$$f = \frac{1}{\sigma} \frac{\int_{\forall} d\forall \int_{t}^{t+T} \varepsilon^2 \left\{ \frac{\nu q^2}{K_p} + \frac{C_f \varepsilon}{K_p} |q|^3 \right\} dt}{\int_{\forall} d\forall \int_{t}^{t+T} \varepsilon q^2 \, dt} \tag{7}$$

The medium parameters in Eq. (7) are determined from steady state tests on small samples of the breakwater material. The velocity field is determined from the theoretical solution. Therefore, an iterative procedure is to be anticipated in the solution to f and q.

Substituting the linearized damping term into Eq. (5) yields the linearized equation of motion

$$\begin{aligned} S \frac{\partial q}{\partial t} &= -\frac{1}{\rho} \nabla (p + \gamma z) - f\sigma q \\ \nabla \cdot q &= 0 \end{aligned} \tag{8}$$

Potential Flow Field

The equation of motion is linear in both q and p. As a result, a simple harmonic excitation will yield a simple harmonic solution to the equation. The excitation in this study is assumed to be a monochromatic sea surface. It is consistent with Eq. (8) to equate the frequency of oscillation within the medium to the frequency of the excitation, σ, so that

$$q(x,y,z,t),\ p(x,y,z,t) = \{q(x,y,z),\ p(x,y,z)\}\ e^{i\sigma t}$$

and

$$\frac{\partial}{\partial t} \{q,p\} = i\sigma \{q,p\}$$

Substituting into Eq. (8) yields

$$(i\sigma S + f\sigma)\ q = -\frac{1}{\rho} \nabla (p + \gamma z)$$

Performing the curl operation on this equation demonstrates the irrotationality of the seepage velocity field, that is

$$\sigma(iS + f)\ \nabla \times q = -\frac{1}{\rho} \nabla \times \nabla (p + \gamma z) = 0$$

Thus, $\nabla \times q = 0$, the flow field is irrotational and a velocity potential, Φ, may be defined wherein

$$q = \nabla\Phi \tag{9}$$

Combining Eq. (9) with the incompressible continuity equation yields Laplace's equation

$$\nabla \cdot q = \nabla \cdot \nabla\Phi = \nabla^2\Phi = 0$$

which must be satisfied throughout the flow field.

Substituting Eq. (9) into (8) and removing the gradient operator leads to

$$S \frac{\partial\Phi}{\partial t} + \frac{1}{\rho}(p + \gamma z) + f\sigma\Phi = 0 \tag{10}$$

This is the linearized unsteady Bernoulli equation for flow in large scale granular media with quasi-linear damping. Along with Laplace's equation, it describes the flow and pressure field within the interstices of the granular media. In order to completely specify the problem, it is necessary to resolve the boundary conditions.

Boundary Value Problem

A vertical section of the solution domain is specified by a horizontal bottom at depth $z = -h$ and a free surface $z = \eta$, referenced to the still water level.

Capillarity and surface tension are negligible phenomena due to the large scale of the pores in media of interest. Consequently, the fluid pressure at the free surface is atmospheric pressure. The dynamic free surface condition is obtained by evaluating the Bernoulli equation at the free surface with $p = 0$ at $z = \eta$, thus

$$\eta = -\frac{1}{g}\left(S \frac{\partial\Phi}{\partial t} + f\sigma\Phi\right)_{z = \eta = 0} \tag{11}$$

where $g = \frac{\gamma}{\rho}$, the acceleration due to gravity. In order to avoid the difficulties of a transcedental solution and in keeping with the small amplitude wave assumption, the surface boundary condition is evaluated at $z = 0$.

The rate at which the free surface rises and falls about the still water lever (SWL), $d\eta/dt$, is equal to the vertical velocity component in a pore at the free surface, $\partial\Phi/\partial z$. This specifies the kinematic free surface condition as

$$\frac{d\eta}{dt} = \frac{\partial\eta}{\partial t} + \frac{\partial\eta}{\partial x}\frac{dx}{dt} = \left.\frac{\partial\Phi}{\partial z}\right|_{z = 0} \tag{12}$$

The convective term is of second order and may be ignored. Substituting Eq. (12) into (11) and applying the simple harmonic time dependence to the velocity potential yields the homogeneous free surface boundary condition

$$\left[g \frac{\partial \Phi}{\partial z} + \sigma^2 \, (if - S)\Phi \right]_{z = 0} = 0 \tag{13}$$

Breakwaters are commonly constructed on natural bottoms of very low permeability (sand, shale or bedrock). It is consistent to regard such a foundation as being impervious. It follows that the vertical velocity component must vanish at z = -h, i.e.,

$$\left. \frac{\partial \Phi}{\partial z} \right|_{z = -h} = 0 \tag{14}$$

Laplace's equation, along with the homogeneous boundary conditions expressed in Eqs. (13) and (14) specify the general form of the boundary value problem.

Throughout the domain: $\nabla^2 \Phi = 0$

At z = 0 : $g \frac{\partial \Phi}{\partial z} + \sigma^2 \, (if - S)\Phi = 0$

At z = -h : $\frac{\partial \Phi}{\partial z} = 0$

General Solution

This study seeks a two dimensional solution to the equations of motion. The longitudinal coordinate is in the direction of incident wave propagation. The homogeneous boundary value problem may be solved using a separation of variables technique. In the absence of a superimposed current, the general solution is

$$\Phi_n = i(a_{1n} e^{-iK_n x} + a_{2n} e^{iK_n x}) \frac{g}{\sigma(S - if)} \frac{\text{ch } K_n(h + z)}{\text{ch } K_n h} e^{i\sigma t} \tag{15}$$

where

$$\sigma^2 (S - if) = gK_n \text{ th } K_n h \tag{16}$$

and ch, th represent the hyperbolic cosine and tangent functions, respectively.

Equation (16) is a characteristic equation which specifies an infinite number of acceptable values to the complex eigen value K_n. For each eigen value, K_n, there is one eigen function, Φ_n, with its own arbitrary constants, a_{1n} and a_{2n}. Each eigen function is a solution to the boundary value problem. The total solution is the sum of all eigen functions. In theory, an infinite number of eigen functions exist, but in practice it is found that only a finite number of eigen functions need be summed to specify a problem to a reasonable degree of accuracy. Thus, the total solution is

$$\Phi = \sum_{n=1}^{\infty} \Phi_n \tag{17}$$

Equation (16) is equivalent to the dispersion equation in linear wave theory. Separating K_n into real and imaginary parts

$$K_n = \Gamma_n (1 - i\alpha_n) \tag{18}$$

and substituting into Eq. (16) yields a pair of dispersion equations for the real quantities Γ_n and α_n.

$$\frac{S\sigma^2}{g} = \Gamma_n \operatorname{th} \Gamma_n h \; \frac{1 - \dfrac{\alpha_n \sin 2\alpha_n \Gamma_n h}{\operatorname{sh} 2\Gamma_n h}}{1 - \dfrac{\sin^2 \alpha_n \Gamma_n h}{\operatorname{ch}^2 \Gamma_n h}} \qquad \frac{f}{S} = \alpha_n \; \frac{1 + \dfrac{\sin 2\alpha_n \Gamma_n h}{\alpha_n \operatorname{sh} 2\Gamma_n h}}{1 - \dfrac{\alpha_n \sin 2\alpha_n \Gamma_n h}{\operatorname{sh} 2\Gamma_n h}}$$

Note that with no damping (f = 0) and no virtual mass effect (S = 1.0), the above reduce to the linear wave theory velocity potential and dispersion equations.

Substitution of Eqs. (15), (16) and (18) into the dynamic free surface condition yields

$$\eta_n = a_{1n} e^{-\alpha_n \Gamma_n x} e^{i(\sigma t - \Gamma_n x)} + a_{2n} e^{\alpha_n \Gamma_n x} e^{i(\sigma t + \Gamma_n x)}$$

Thus, the surface profile is composed of a series of exponentially damped sinusoids propagating in both the positive and negative x directions. The real part of the complex wave number, Γ_n, specifies the spatial periodicity while the imaginary part, α_n, specifies the decay rate.

Vertical Face Breakwaters

The two dimensional velocity potential described by Eq. (15) applies to a media of finite depth and arbitrary longitudinal extent. To specify the potential for a breakwater of finite width, b, consider a crib style breakwater, located in a monochromatic sea environment, as sketched in Fig. 1. As an incident wave encounters the breakwater face at x = 0, a reflected wave is formed and a wave propagates through the structure to x = b where it is partially reflected, partially transmitted.

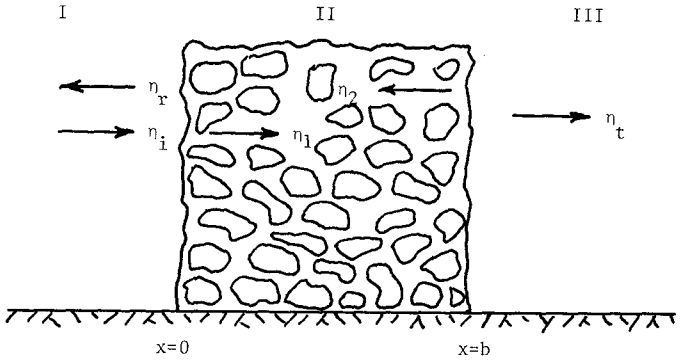

Figure 1. Crib Style Breakwater

A series of eigen modes is generated in each of the four resulting wave trains. Linear wave theory applies in regions I and III where f = 0 and S = 1.0. In these two regions, only the progressive modes propagate away from the breakwater. The local modes, characterized by imaginary wave numbers, are necessary to satisfy the interfacial boundary conditions but decay rapidly away from the breakwater.

The general solutions in each of the three regions are known. To apply the general solutions to this particular problem, the phase of the unknown amplitudes must be referenced appropriately. The incident, reflected and positively directed interior waves are referenced to the x = 0 face. The transmitted and negatively directed interior waves are referenced to the x = b face. A summary of the solutions, in terms of unknown amplitudes is given below.

Region I

$$\Phi_I = \Phi_i + \sum_{n=1}^{\infty} \Phi_{rn}$$

$$\Phi_i = i\, a_i e^{-ik_1 x} \frac{\sigma}{k_1} \frac{\operatorname{ch} k_1(h+z)}{\operatorname{sh} k_1 h} e^{i\sigma t}$$

$$\Phi_{rn} = i a_{rn} e^{ik_n x} \frac{\sigma}{k_n} \frac{\operatorname{ch} k_n(h+z)}{\operatorname{sh} k_n h} e^{i\sigma t}$$

$$\frac{p_I}{\rho} = -i\sigma\Phi_I - gz \quad , \qquad \sigma^2 = gk_n \operatorname{th} k_n h$$

Region II

$$\Phi_{II} = \sum_{n=1}^{\infty} \Phi_n$$

$$\Phi_n = i(a_{1n}e^{-iK_n x} + a_{2n}e^{iK_n(x-b)}) \frac{\sigma}{K_n} \frac{\text{ch } K_n(h+z)}{\text{sh } K_n h} e^{i\sigma t}$$

$$\frac{p_{II}}{\rho} = -(iS + f)\Phi_{II} - gz \quad , \quad \sigma^2 (S - if) = gK_n \text{th } K_n h$$

Region III

$$\Phi_{III} = \sum_{n=1}^{\infty} \Phi_{tn}$$

$$\Phi_{tn} = ia_{tn}e^{-ik_n(x-b)} \frac{\sigma}{k_n} \frac{\text{ch } k_n(h+z)}{\text{sh } k_n h} e^{i\sigma t}$$

$$\frac{p_{III}}{\rho} = -i\sigma\Phi_{III} - gz \quad , \quad \sigma^2 = gk_n \text{ th } k_n h$$

These equations contain 4n unknowns, i.e., n unknowns for each of the amplitude series a_{rn}, a_{1n}, a_{2n} and a_{tn}. In order to evaluate these unknowns, 4n additional boundary conditions are needed. Since the solutions in adjacent regions must be continuous at the interface between regions, it is apparent that the appropriate boundary conditions are continuity of pressure and horizontal mass flux at x = 0 and x = b. In equation form, the boundary conditions may be summarized as:

x = 0

$$u_I = \varepsilon u_{II} \quad \text{or} \quad \frac{\partial \Phi_I}{\partial x} = \varepsilon \frac{\partial \Phi_{II}}{\partial x}$$

$$p_I = p_{II} \quad \text{or} \quad \Phi_I = (S - if)\Phi_{II}$$

x = b

$$\varepsilon u_{II} = u_{III} \quad \text{or} \quad \varepsilon \frac{\partial \Phi_{II}}{\partial x} = \frac{\partial \Phi_{III}}{\partial x}$$

$$p_{II} = p_{III} \quad \text{or} \quad (S - if)\Phi_{II} = \Phi_{III}$$

Applying the above conditions directly yields a 4n x 4n complex matrix when evaluated at n different values of the depth, z. Considerable simplification may be gained by utilizing the orthogonal properties of the eigen functions. Orthogonality is the characteristic that the integral of the product of two eigen functions vanishes over the limits of the vertical domain if the eigen values are not equal, that is

$$\int_{-h}^{0} \Phi_m \Phi_n \, dz = 0, \; m \neq n$$

It is the z dependent terms that are orthogonal. To utilize this property, the interfacial boundary conditions are multiplied through by ch $K_m(h + z)$

and integrated over the full depth. The results, after much algebraic manipulation, are given below:

$$\sum_{n=1}^{\infty} C_{rn} \frac{K_m^2 - k_1^2}{K_m^2 - k_n^2} \left(\frac{k_n}{k_1} + \frac{\varepsilon}{S - if} \frac{K_m}{k_1} \right) +$$

$$e^{-iK_m b} \sum_{n=1}^{\infty} C_{tn} \frac{K_m^2 - k_1^2}{K_m^2 - k_n^2} \left(\frac{k_n}{k_1} - \frac{\varepsilon}{S-if} \frac{k_m}{k_1} \right) = 1.0 - \frac{\varepsilon}{S-if} \frac{K_m}{k_1}$$

$$\sum_{n=1}^{\infty} C_{rn} \frac{K_m^2 - k_1^2}{K_m^2 - k_n^2} \left(\frac{k_n}{k_1} - \frac{\varepsilon}{S-if} \frac{K_m}{k_1} \right) +$$

$$e^{-iK_m b} \sum_{n=1}^{\infty} C_{tn} \frac{K_m^2 - k_1^2}{K_m^2 - k_n^2} \left(\frac{k_n}{k_1} + \frac{\varepsilon}{S-if} \frac{K_m}{k_1} \right) = 1.0 + \frac{\varepsilon}{S-if} \frac{K_m}{k_1}$$

$$C_{1m} = \frac{S-if-1}{\varepsilon} \frac{k_1 K_m}{K_m^2 - k_1^2} \frac{sh\, K_m h\, ch\, K_m h}{sh\, K_m h\, ch\, K_m h + K_m h} \{1.0 +$$

$$\frac{\varepsilon}{S-if} \frac{K_m}{k_1} - \sum_{n=1}^{\infty} C_{rn} \frac{K_m^2 - k_1^2}{K_m^2 - k_n^2} \left(\frac{k_n}{k_1} - \frac{\varepsilon}{S-if} \frac{K_m}{k_1} \right) \}$$

$$C_{2m} = \frac{S-if-1}{\varepsilon} \frac{k_1 K_m}{K_m^2 - k_1^2} \frac{sh\, K_m h\, ch\, K_m h}{sh\, K_m h\, ch\, K_m h + K_m h} \{$$

$$- \sum_{n=1}^{\infty} C_{tn} \frac{K_m^2 - k_1^2}{K_m^2 - k_n^2} \left(\frac{k_n}{k_1} - \frac{\varepsilon}{S-if} \frac{K_m}{k_1} \right) \}$$

where $C_{rn}, C_{1n}, C_{2n}, C_{tn} = \frac{a_{rn}}{a_i}, \frac{a_{in}}{a_i}, \frac{a_{2n}}{a_i}, \frac{a_{tn}}{a_i}$

A brief inspection of the above equations reveals that the solution has been reduced to a 2n x 2n complex matrix for the dimensionless amplitudes of the reflected and transmitted waves and two linear vector equations for the dimensionless amplitudes inside the breakwater. It is apparent from the terms appearing in these last four equations that the solution ultimately depends on: the structural properties of the breakwater width and depth, b and h; the media properties of porosity and damping, ε and f; and the wave properties as described by the wave numbers inside and outside the breakwater, K_n and k_n.

Long Wave Solution

The complete solution is difficult to interpret qualitatively because of the series form of the complex matrix. Some insights into the general solution behavior may be gained, however, by considering the relatively simple case of long wave excitation. This condition is attained when the wave length exceeds the water depth by a factor of twenty so that the hyperbolic and trigonometric functions are equivalent to the values of their respective arguments. Then the dispersion equations become

$$\frac{\sigma^2 h}{g} = k_n h \, \text{th} \, k_n h \cong (kh)^2$$

$$\frac{\sigma^2 h}{g} (S - if) = K_n h \, \text{th} \, K_n h \cong (Kh)^2 \qquad (19)$$

Each equation reduces to a single positive root and the depth dependence drops from the equations of motion. Only a single eigen value exists for the solution in each of the three regions prescribed in Fig. 1. Thus, the total solution reduces to one component in each of the four unknown wave trains.

Substituting $Kh = \Gamma h(1-i\alpha)$ into Eq. (19) and separating real and imaginary parts yields

$$\Gamma^2 h^2 = \frac{1}{2} \frac{\sigma^2 h}{g} S \left(1 + \sqrt{1 + f^2/s^2}\right), \quad \alpha = \frac{\sqrt{1 + f^2/S^2} - 1}{f/S} \qquad (20)$$

Note that the effect of the damping coefficient, f, is to increase the long wave number inside the breakwater relative to its value outside. This causes the wave length to shorten, a result which one might anticipate. In general, friction inhibits wave propagation, therefore the celerity and wave length should be decreased, as indicated by Eq. (20).

The breakwater depth and width are of the same order of magnitude so that small Kh implies small Kb. Utilizing the small argument identities for the hyperbolic and trigonometric functions and evaluating the general series solution for a single eigen value yields the following for the dimensionless long wave complex amplitudes:

$$C_r = \frac{S - if - \varepsilon^2}{S - if + \varepsilon^2 - i2\varepsilon \frac{\sqrt{gh}}{\sigma b}} \qquad C_t = \frac{1}{1 + \frac{i}{2\varepsilon} \frac{\sigma b}{\sqrt{gh}} (S - if + \varepsilon^2)}$$

$$C_1 = \frac{\left(1 + \frac{\sqrt{S-if}}{\varepsilon}\right)\left(1 + \frac{i\sigma b}{\sqrt{gh}} \sqrt{S-if}\right)}{2 + \frac{i}{\varepsilon} \frac{\sigma b}{\sqrt{gh}} (S - if + \varepsilon^2)} \qquad C_2 = \frac{1 - \frac{\sqrt{S-if}}{\varepsilon}}{2 + \frac{i}{\varepsilon} \frac{\sigma b}{\sqrt{gh}} (S - if + \varepsilon^2)} \qquad (21)$$

These equations represent an exact solution to the permeable break-

water problem for the specific case of an incident wave which is very long with respect to water depth and breakwater width. The simple form of the equations allows one to easily interpret the effect of various independent parameters on the solution. Some pertinent limiting conditions are: As the medium takes on the properties of pure sea water, i.e., 100% porosity and no damping, transmission becomes complete and no reflection occurs ($f \to 0$, $\varepsilon \to 1$ with $S = 1$ yields $C_t \to 1$, $C_r \to 0$). As the porosity approaches zero, the breakwater assumes the characteristic of a solid vertical wall and no transmission occurs while reflection becomes perfect ($\varepsilon \to 0$ yields $C_t \to 0$, $C_r \to 1$). As the damping properties of the medium become severe (either inertial or dissipative) the transmission drops to zero and the reflection becomes perfect (f or $S \to \infty$ yields $C_t \to 0$, $C_r \to 1$). As the breakwater becomes very thin, the transmission becomes nearly complete while the reflection becomes negligible ($b \to 0$ yields $C_t \to 1$, $C_r \to 0$). Finally, as the wave period becomes very long, such as a tidal oscillation, the transmission becomes complete and no reflection occurs ($\sigma \to 0$ yields $C_t \to 1$, $C_r \to 0$. These same trends have been observed in the solution to the general problem for shorter waves.

Equation (21) verifies that increasing the friction coefficient, f, or the product of f with the wave frequency, σ, causes a relative decrease in the long wave transmission coefficient. This behavior also applies to the short wave solution. It will be useful, therefore, to be able to predict the dependence of $f\sigma$ on the wave and breakwater characteristics. Lorentz's condition of equivalent work, as given by Eq. (7) specifies this dependence. The friction coefficient characterizes the damping throughout the breakwater so the volume integral in Eq. (7) may be replaced by a double integral on x and z with the submerged portion of the breakwater as limits of integration.

$$f\sigma = \frac{\int_{h}^{0} dz \int_{0}^{b} dx \int_{t}^{t+T} \varepsilon^2 \left\{ \frac{\nu q_R^2}{K_p} + \frac{C_f \varepsilon}{\sqrt{K_p}} \left| q_R \right|^3 \right\} dt}{\int_{-h}^{0} dz \int_{0}^{b} dx \int_{t}^{t+T} \varepsilon q_R^2 \, dt} \qquad (22)$$

where q_R is the real part of the complex velocity, q. The numerator includes a term which is proportional to the cube of the velocity whereas the denominator is proportional to the square of the velocity. Consequently, relative increases in the velocity will cause relative increases in $f\sigma$. The velocity inside the breakwater is proportional to the product of the wave amplitude and wave frequency. The amplitude and frequency of the wave components inside the breakwater increase monotonically with increasing amplitude and frequency of the incident wave. Consequently, if the wave frequency is held constant then a relative increase in the incident amplitude will cause a relative increase in $f\sigma$. Likewise, if the amplitude is held constant, then a relative increase in the frequency, i.e., decrease in period and wave length, will cause an increase in $f\sigma$. Since increasing $f\sigma$ causes a decrease in the transmission coefficient it may be concluded that the transmission coefficient will decrease for increasing wave steepness or increasing wave number.

Solution Method

The solution method is a straight forward iterative technique. An outline of the procedure is given below.

1) Assume an initial value for f, e.g., f = 1.0.
2) Solve the dispersion equation, (16), for n eigen values. n ≈ 5 yields better than 95% convergence for kh ≤ π.
3) Solve the complex matrix for the amplitude and phase of n-modes in each unknown wave train.
4) From 3) determine q and solve the Lorentz equation, (22), for f.
5) Compare the calculated f with the assumed f and iterate if necessary (return to 2)).
6) The absolute values of C_r and C_t are the reflection and transmission coefficients for the structure.

The iteration scheme typically closes after two to eight cycles and is efficiently performed on a digital computer.

Conventional Breakwater Schemes

The preceding discussion has been limited to permeable structures of rectangular form. The inclusion of layered, trapezoidal shaped breakwaters greatly complicates the problem. A rigorous analytical solution is virtually impossible due to the non-homogeneous boundary conditions and wave breaking which occurs at the inclined breakwater slopes. To circumvent these difficulties this study introduces an approximate equivalent rectangular breakwater solution.

The simplified approach replaces the actual structure with an equivalent rectangular breakwater which has the same submerged volume as that of the trapezoidal breakwater. That is, a hypothetical breakwater is formed by bisecting the slopes between z = 0 and z = -h with vertical planes, as in Fig. 2. Within the confine of these planes, the rectangular breakwater has the same internal structure as the trapezoidal breakwater, and the crib style breakwater solution of the previous section is used to describe the flow field. Exterior to these planes, linear wave theory is applied to describe the incident, reflected and transmitted wave trains. The two solutions are matched at the hypothetical interfaces to satisfy continuity of pressure and horizontal mass flux and thereby solve for the unknown modal amplitudes.

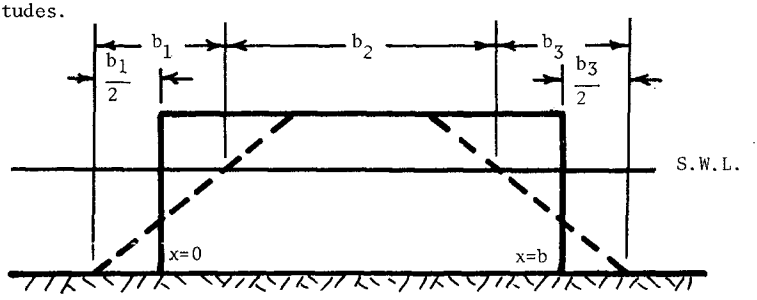

Figure 2. Equivalent Rectangular Breakwater

Lorentz's condition of equivalent work is used to evaluate a linearized damping coefficient, f, which applies throughout the hypothetical rectangular breakwater. However, unlike the condition derived for the crib style breakwater, the new equivalent work principle attempts to account for the effect of energy dissipation due to wave breaking on the windward slope. This is accomplished by modifying a theory attributed to Miche (1951) which estimates the wave energy losses on impermeable slopes. These losses are added to the frictional losses in the numerator of Eq. (22) to yield a revised estimate to the damping coefficient, f. Thus,

$$f\sigma = \frac{\int_{h}^{0} dz \int_{0}^{b} dx \int_{t}^{t+T} \varepsilon^2 \left\{ \frac{\nu q_R^2}{K_p} + \frac{C_f \varepsilon}{\sqrt{K_p}} |q_R|^3 \right\} dt + \frac{\dot{\bar{E}}_{loss}}{\rho}}{\int_{-h}^{0} dz \int_{0}^{b} dx \int_{t}^{t+T} \varepsilon q_R^2 \, dt} \qquad (23)$$

where $\dot{\bar{E}}_{loss}$ is the period averaged power lost to breaking. In this manner surface breaking losses are combined with internal friction losses. The effect is distributed among the various modal components in the reflected and transmitted wave trains through the dependence of the interfacial boundary conditions on f.

The details required to evaluate $\dot{\bar{E}}_{loss}$ are presented in the reference by Sollitt and Cross (1972). The calculation is empirical but facilitates enumeration of breaking losses in the absence of precise analytical methods. As improved methods become available, they may be incorporated into the calculation. The intent of the present discussion is to identify the concept and relegate the mechanical details to the parent reference.

Summarizing, the conventional sloping face breakwater problem is solved by adding breaking losses to the crib style breakwater solution. This effectively increases the friction coefficient f and reduces the transmission coefficient accordingly.

Experimental Results

Experimental results for two model breakwater configurations are presented. The first model is a homogenous, vertical walled breakwater composed of 3/4" gravel contained in a wire screen crib. The model is twelve inches wide and extends well above the height of maximum clapotis. The water depth is twelve inches.

The second model is a layered trapezoidal shaped structure dimensioned as in Fig. 3. The media properties are also tabulated in the figure. The properties of the second layer correspond to those of the crib style breakwater as well.

A complete documentation of the experimental program is presented in the reference by Sollitt and Cross (1972). Sample results are presented in the following figures. The crib style breakwater behavior is displayed in Figs. 4 and 5. The trapezoidal layered breakwater behavior is displayed in Figs. 6 and 7. The reflection and transmission coefficients are presented as functions of wave steepness and wave number. A dominant feature is the

decrease in the transmission coefficient with increasing wave steepness. This characteristic is due to non-linear damping as predicted by the theory. The reflection coefficient is relatively insensitive to wave steepness for the crib style breakwater case but decreases due to wave breaking on the sloping face breakwater. The reflection and transmission coefficients decrease with increasing wave number (decreasing wave length) for both configurations.

Comparison of Theory and Experiment

The theory is evaluated using the given breakwater properties and five terms in the eigen series solution. The virtual mass coefficient, C_M, is unknown and is taken equal to zero by default. Theoretical reflection and transmission coefficients are solved using the iteration procedure discussed previously. The results are presented as continuous and dashed lines on the experimental plots.

Figures 4 and 5 reveal that the theory tends to underestimate the reflection coefficient and slightly overestimate the transmission coefficient for the crib style breakwater. The correlation is improved by taking non-zero values for the virtual mass coefficient. One cannot predict the magnitude of this coefficient apriori because the virtual mass of densely packed fractured stone is not known. Evaluation of C_M, however, may serve as a calibrating link between theory and experiment in future studies.

Theory and experiment also tend to diverge for very small values of the incident wave amplitude in both models. This response is apparent at small H_i/L on the constant kh curves, and at large kh on the constant H_i/L curves. It can be shown that this occurs when the scale of the fluid motion becomes smaller than the aggregate scale on the breakwater surface. As the wave amplitude becomes very small, the wave field orbit diameters are exceeded by the individual rock diameters on the slope. Then the waves begin interacting with individual pieces of gravel rather than a continuous porous slope. The reflection process is modified as waves are partially reflected directly off particle surfaces and the theoretical assumption of a continuum no longer applies.

Correlation between the conventional trapezoidal shaped breakwater theory and experiment is quite favorable. The results, however, are contingent upon proper evaluation of the breaking losses, and further insights into the breaking process are needed.

Conclusions

Theory and experiment for both breakwater configurations generally concur that: 1) the transmission coefficient decreases with decreasing wave length, breakwater porosity and permeability, and increasing wave height and breakwater width. 2) The reflection coefficient decreases with decreasing breakwater width and wave length and increasing porosity and permeability.

Correlation between experiment and theory is best when the incident wave height exceeds the particle diameter of the medium. Although additional work is needed to improve the breaking wave calculation, the predicted reflection and transmission coefficients are very useful design estimates.

Acknowledgements

The study was conducted at the Massachusetts Institute of Technology and sponsored by the U.S. Army Coastal Engineering Research Center.

References

Calhoun, R. J., "Field Study of Wave Transmission Through a Rubble Mound Breakwater", M.S. Thesis, U.S. Navy Postgraduate School, March 1971

Cross, R. H., Sollitt, C. K., "Wave Transmission by Overtopping", Massachusetts Institute of Technology, Hydrodynamics Laboratory Technical Note No. 15, July 1971

Miche, M., "Pouvoir Réfléchissant des Ouvrages Maritimes Exposes a l'Action de Houle", Annales des Ponts et Chaussees, May-June 1951, pp. 285-319

Sollitt, C. K., Cross, R. H., "Wave Reflection and Transmission at Permeable Breakwaters", Massachusetts Institute of Technology, R. M. Parsons Laboratory Technical Report No. 147, March 1972

Ward, J. C., "Turbulent Flow in Porous Media", Proc. ASCE, J. Hyd. Div., Vol. 90, No. HY 5, Sept. 1964, pp. 1-12

Layer	ϵ	C_f	K_p	diam.
1	0.434	0.282	$0.482 \cdot 10^{-5}$	1.37"
2	0.439	0.295	$0.1138 \cdot 10^{-5}$	0.774"
3	0.430	0.4056	$0.375 \cdot 10^{-6}$	0.382"

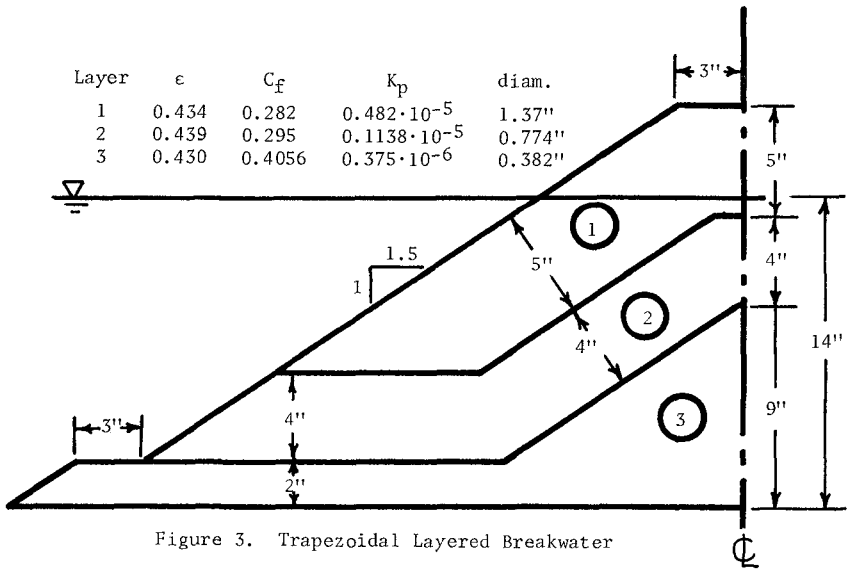

Figure 3. Trapezoidal Layered Breakwater

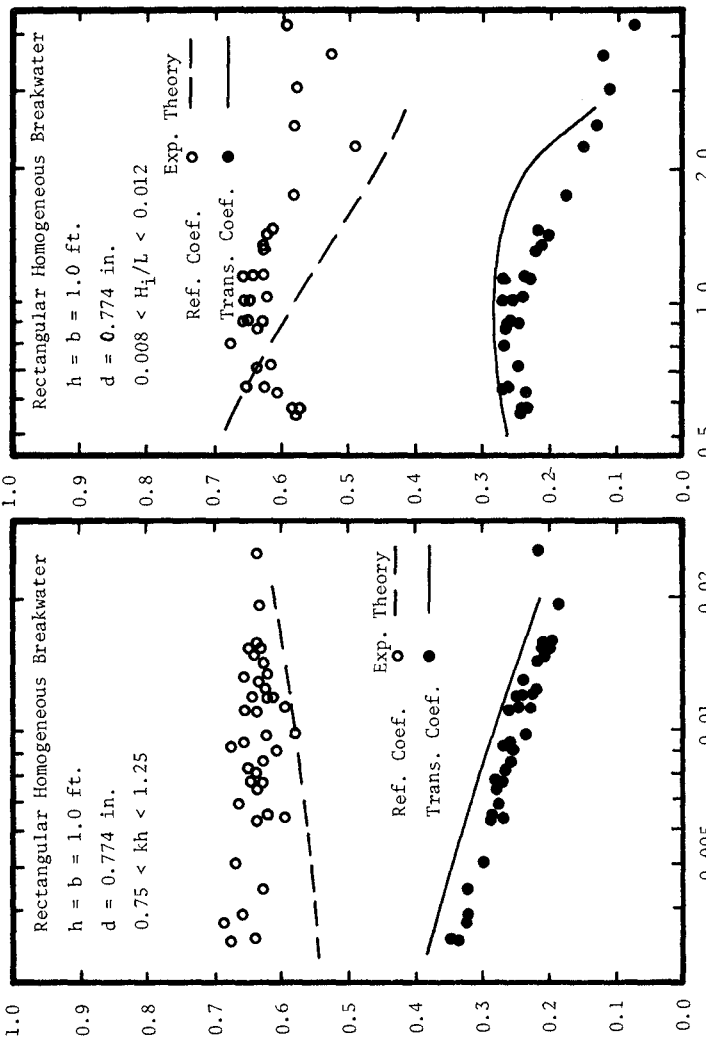

Figure 4. Reflection, Transmission Coefficient Dependence on Wave Steepness

Figure 5. Reflection, Transmission Coefficient Dependence on Wave Number

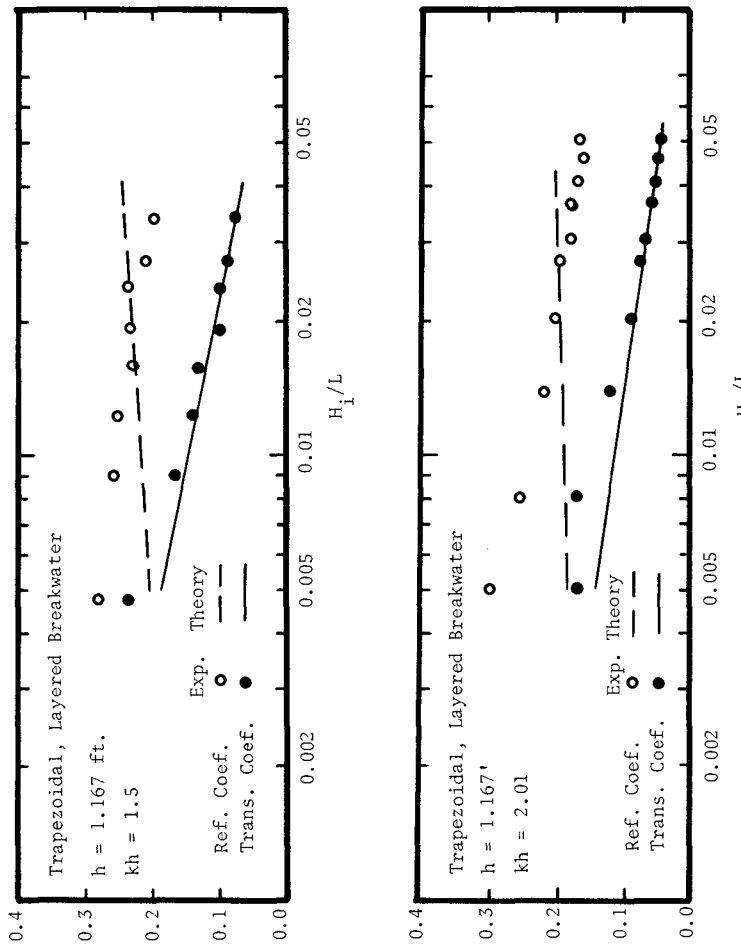

Figure 6. Reflection, Transmission Coefficient Dependence on Wave Steepness

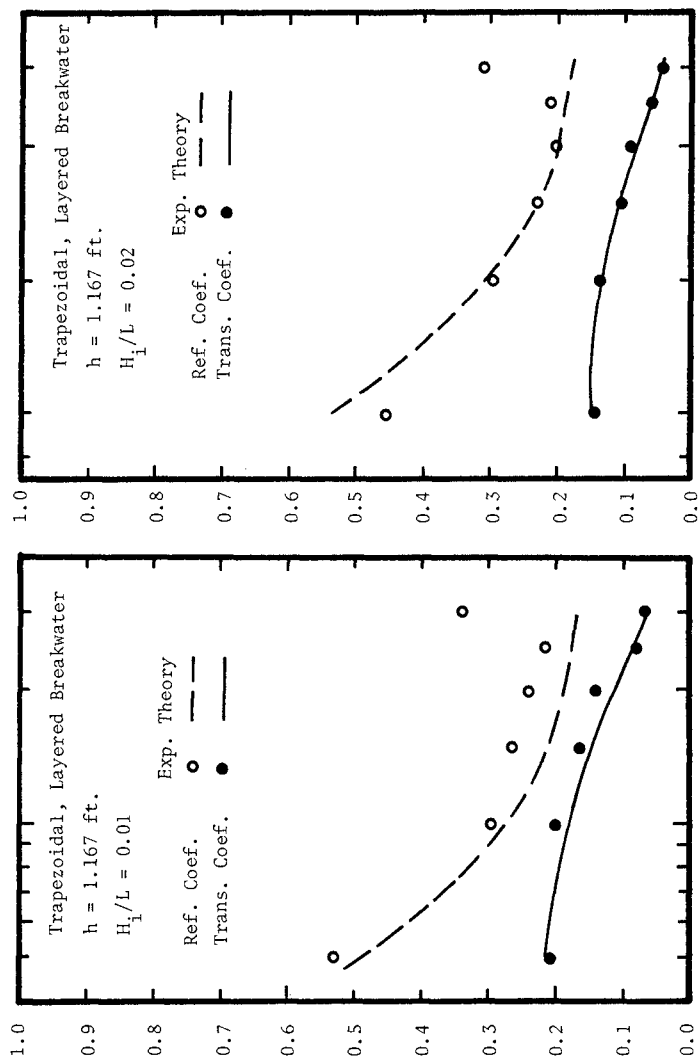

Figure 7. Reflection, Transmission Coefficient Dependence on Wave Number